





beamline was evaluated by comparing the reactions  $n+Al \rightarrow {}^7Be+X$  and  $n+Al \rightarrow {}^{22}Na+X$ . The contamination amounted to  $\sim 20\%$ , and was added to the proton fluence. The fluence over the detector plane was uniform to 14% and 5% in the first and second irradiations, respectively.

### III. PERFORMANCE RESULTS

#### A. Damage to coupling capacitors

The coupling capacitors could potentially be damaged by intense radiation during the ATLAS experiment. Although the readout strips are held at ground in the ATLAS SCT design, large leakage current after radiation damage will be routed to the preamplifier if the damaged capacitor turns to be shorted.

The coupling capacitors of the detectors irradiated to  $1.7 \times 10^{14}$  protons/cm<sup>2</sup> were measured at 1 kHz with applying 5 V across the aluminum strip and the implant strip underneath. No reverse bias voltage was applied to the bulk. We defined faulty capacitors if the capacitance is off by more than 25% from the average. Table 2 lists the numbers of faulty capacitors and the average capacitances before and after irradiation. Most of the faulty capacitors after irradiation were faulty at pre-irradiation measurement, and quite a few faulty capacitors were created by irradiation (see numbers in parentheses in the table). Except for some capacitors of Sp4k-17 and Hn4kID-17, which became nearly shorted, most of the damaged capacitors are still usable.

The average capacitances are found to increase for p-strip and decrease for n-strip detectors. Negative charge induced nearby the implant electrodes effectively widens the electrode, so it can influence the capacitance measurement, which explains the increase observed for p-strip detectors. For n-strip detectors on the other hand, negative charge around the implant strips is swept away after the ohmic n<sup>+</sup>-n contact side changed to n<sup>+</sup>-p junction side.

Table 2

Summary of numbers of faulty coupling capacitors measured before and after irradiation. The numbers of faulty capacitors created by irradiation are shown in parentheses. The errors of pre-irradiated detectors are rms spreads.

Detector	#bad strips		Capacitance (pF)	
	Before	After	Before	After
Hp4k-17	0	4 (4)	131±3	+10
	0	0 (0)	132±2	+10
Hp1k-17	0	0 (0)	117±4	+17
	2	2 (0)	121±6	+26
Sp4k-17	5	4 (2)	151±14	+18
	0	8 (8)	148±16	+19
Hn4kFC-17	6	6 (0)	144±21	-6
	5	5 (0)	129±20	-5
Hn4kID-17	18	21 (6)	148±26	-8
	11	10 (1)	145±20	-6
Hn4kIA-17	1	1 (0)	143±5	-5
	1	1 (0)	133±7	-3
Hn4kIB-17	2	2 (0)	142±6	-4
	1	1 (0)	137±5	-6

We note that large rms spreads of n-on-n detectors are due to some of the faulty capacitors and the spreads of genuine capacitors are quite similar among the Hamamatsu detectors. The coupling capacitances of the two SINTEF detectors turned to be smaller near the end strips by at maximum 40%. The faulty capacitances for SINTEF were defined by 25% deviation from the local average taking into account of the structure over the strips.

#### B. I-V and C-V characteristics

The I-V and C-V characteristics of the samples irradiated to  $4.2 (1.7) \times 10^{14}$  protons/cm<sup>2</sup> were measured 16 (10) months after the irradiation was completed. The detectors were kept at 0°C in a refrigerator but taken out for typically a few hours in preparation at room temperature for charge collection measurement described in the next section. The detectors irradiated to  $4.2 \times 10^{14}$  protons/cm<sup>2</sup> were in addition kept for 5 days at room temperature and 7 days at 28°C [3].

The full depletion voltage of irradiated samples show annealing at first and then anti-annealing because of different time scales involved in these processes [5]. A calculation results that the both sets of samples have experienced the first annealing and the samples irradiated to  $4.2 \times 10^{14}$  protons/cm<sup>2</sup> have increased the full depletion voltage by about 25%.

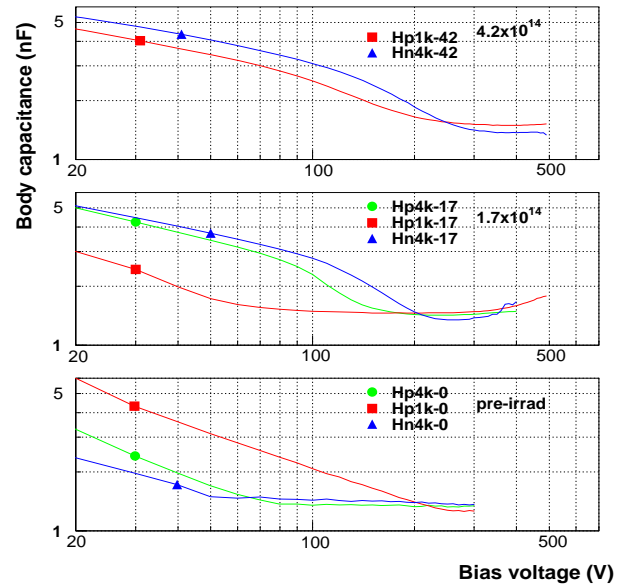


Figure 2: C-V characteristics of Hamamatsu Hp4k, Hn4kID and Hp1k detectors, measured at pre-irradiation and after  $1.7 \times 10^{14}$  and  $4.2 \times 10^{14}$  protons/cm<sup>2</sup>.

The body capacitance was measured at a frequency of 1 kHz. The post-irradiation measurements were made at  $-30^\circ\text{C}$  in order to keep the total leakage current small while the pre-irradiation measurements were at room temperature. Figures 2 and 3 show the C-V and I-V curves of samples Hp4k, H4nk and Hp1k. For ideal planer diodes the body capacitance is expected to decrease with bias voltage as  $V^{-0.5}$  until the bulk is fully depleted, as can be seen in the data before irradiation. The C-V curves of irradiated detectors, however, show different characteristics: C decreases as  $V^{-0.5}$  at low voltages and then steeper before the capacitance becomes constant. Similar tendency was observed for other detectors. The C-V

characteristics at  $1.7 \times 10^{14} \text{ cm}^{-2}$  clearly shows that detectors with  $1 \text{ k}\Omega\text{cm}$  reach the plateau at voltage lower than Hp4k and Hn4k. However, since the full depletion voltage can not be extracted reliably from such curves, other standard is setup in the next chapter to evaluate the relevant voltage to compare.

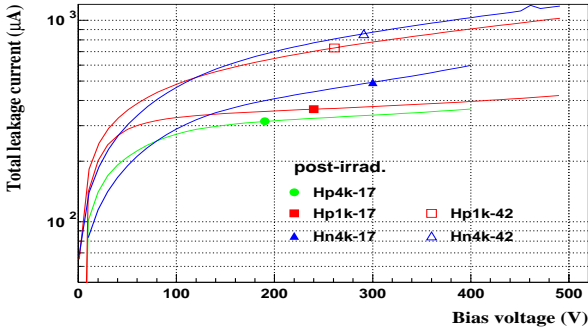


Figure 3: I-V characteristics of Hamamatsu Hp4k, Hn4kID and Hp1k detectors (post-irradiation measurement). The leakage current is expressed at  $-10^\circ\text{C}$ .

The leakage current at  $-10^\circ\text{C}$  is typically  $300\text{--}400 \mu\text{A}$  at  $200 \text{ V}$  after  $1.7 \times 10^{14} \text{ protons/cm}^2$  and  $800\text{--}900 \mu\text{A}$  at  $300 \text{ V}$  after  $4.2 \times 10^{14} \text{ protons/cm}^2$ . It is not clear at this stage at which voltages the leakage currents should be compared: The above voltages are those determined from the charge collection curves, as discussed in the next chapter. The leakage current is proportional to the proton fluence after taking into account the anti-annealing effects in the depletion voltage for the samples irradiated to  $4.2 \times 10^{14} \text{ protons/cm}^2$ .

### C. Charge Collection

The bias voltage relevant at operation should be evaluated from the charge collection efficiency. We have carried out the measurement using a  $^{90}\text{Sr}$   $\beta$  source. Signals out of three neighboring strips were fed separately into CAMAC ADCs through low-noise preamplifiers HIC-1576 [12] and shapers with  $200 \text{ ns}$  shaping time. A pair of  $300 \mu\text{m}$  wide and  $10 \text{ mm}$  long slits were machined in  $5 \text{ mm}$  thick aluminum plates and were aligned along the center strip with placing the detector in between. The ADC gate was generated by a scintillating counter set underneath the bottom slit. Several aluminum electrodes besides the three readout strips were wire-bonded to ground.

The detector and preamplifier were placed in a thermostat chamber and cooled to  $-30^\circ\text{C}$ . Figure 4 shows typical pulse height distributions of the three channels. The distributions before selection are evident for pedestals (around 100 counts) and signals (around 450). In order to ensure that  $\beta$  rays passed through the center strip, we required that the signal out of the center strip was maximal in an event. With this selection, only the center strip shows a peak while the strip at neighbor shows a pedestal and tail which corresponds to the case where the track was shared between the two. The three ADC counts were then summed with the selection applied, and the peak was derived by fitting a Gaussian function with asymmetric variances around the peak. The peak positions as a function of bias voltage are plotted in Figure 5 for some detectors. The voltage and charge values are corrected for the detector thickness and expressed for  $300 \mu\text{m}$  thickness. The ordinate is then normalized by the plateau in the charge collection curve

of Hp4k-0 detector. Among the above samples, Hn4kID-42 showed large noise and the peak was not reliably determined at above  $400 \text{ V}$ . Sp4k-42 showed the peak increasing up to  $500 \text{ V}$ , which was the maximum our equipment was able to supply.

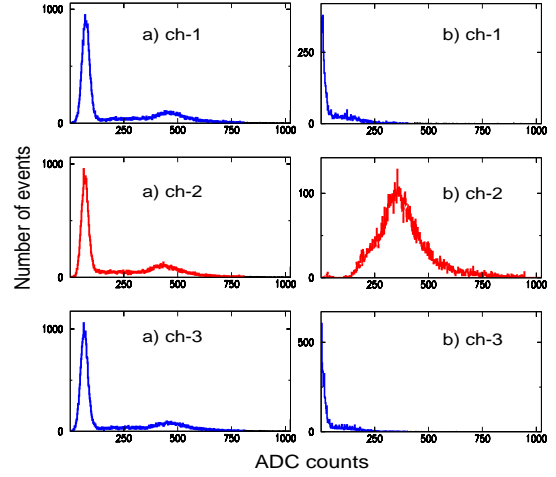


Figure 4: Charge distributions out of three neighboring strips (a) without any selection and (b) with selection described in the text. In b), pedestals are subtracted.

We evaluated the absolute charge scale by comparing the pulse height to  $\beta$  rays with the  $60 \text{ keV}$  photoelectric peak of  $^{241}\text{Am}$   $\gamma$ 's. We assumed the energy of  $3.6 \text{ eV}$  to create an electron-hole pair in silicon. The calibrated pulse height for  $\beta$  rays was  $3.2 \text{ fC}$  per  $300 \mu\text{m}$  after correcting for detector thickness and the  $\beta$  ray angle.

After  $1.7 \times 10^{14} \text{ cm}^{-2}$ , there is small difference between initial p-on-n (Hp4k-17) and n-on-n (Hn4k-17) detectors in the shapes of the charge collection curves though the maximum collected charge is smaller by  $\sim 10\%$  for initial p-on-n detectors. The pre-irradiation detectors show that the collected charge drops quickly for n-on-n detectors at low voltage, which is explained by the fact that the readout strips are not well isolated electrically. Despite the fact that reading out is on the ohmic side for irradiated p-strip detectors, the charge collection at low voltages is not much degraded. Negative charge accumulated between the p-strips functions as to isolate them and the regions around the strips may be preferentially depleted at lower voltage. At higher voltages the region between strips is gradually depleted. As we have seen, C-V curves of irradiated p-strip detectors show two slopes to be fully depleted. The two structures in the C-V curves may correspond to the two depletion processes mentioned here.

The difference between Hp1k-17 and Hp4k-17 is evident, while the difference in shape becomes small between Hp1k-42 and Hn4k-42. Although we have no sample of  $4 \text{ k}\Omega\text{cm}$  p-on-n detectors irradiated to  $4.2 \times 10^{14} \text{ protons/cm}^2$ , the difference due to bulk resistivity is probably small at this fluence for the similarity in shape between p-on-n and n-on-n detectors at  $1.7 \times 10^{14} \text{ protons/cm}^2$ . In the fluence range below  $\sim 2 \times 10^{14} \text{ protons/cm}^2$ , the higher initial donor impurity can compensate the radiation created acceptors and use of low resistivity wafer



may have the possibility to enlarge the safety margin in the detector operation.

The charge collection curve of Hp4km-17, manufactured in the modified process, is shifted to lower voltage than that of Hp4k-17. The maximum collected charges of these two samples agree with each other within  $\sim 10\%$ .

Comparing to Hamamatsu Hp4k detectors, SINTEF detectors showed consistently larger voltages by  $\sim 20\%$  to turn to the plateau. The maximum collected charges at  $1.7 \times 10^{14} \text{ cm}^{-2}$  is somewhat smaller but are consistent at  $4.2 \times 10^{14} \text{ cm}^{-2}$ .

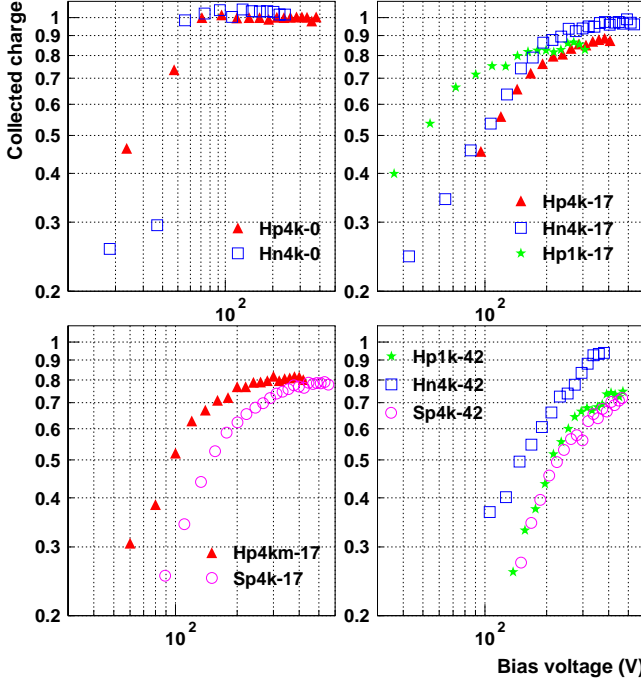


Figure 5: Charge collection as a function of bias voltage. The ordinate is normalized by maximum collected charge of Hp4k-0, 3.2 fC.

#### D. Front-biasing

In Hamamatsu detectors a wide  $n^+$  is implanted in the edge region surrounding the entire sensitive area. Aluminum electrodes are DC connected to the  $n^+$  implant through the  $\text{SiO}_2$  layer. This design minimizes the effects on leakage current increase from the scribed edges and from environment. The same aluminum electrode can be biased to fully deplete the detector through  $n^+$ - $n^+$  ohmic contact to the backplane.

If such an electrode is usable also for irradiated detectors, the biasing scheme can be simplified: conductive epoxy or wire-bonding to the backplane can be avoided. The resistance between the front electrode and backplane is, though, expected to increase after bulk inversion since reverse biasing is required across  $n^+$ -p junction. We have measured the bulk resistance near the edge in a configuration shown in Figure 6. With applying positive voltage (source voltage  $V_s$ ) on the edge electrode with respect to the bias-ring, the voltage across the edge electrode to the backplane ( $V$ ) was measured. The current  $I_0$  generated by  $V_s$  is collected through  $n^+$ -(inverted p)- $n^+$  and partially through the surface. Therefore, the edge resistance  $R$  is equal to or greater than  $R_0$  defined as the ratio of  $V$  and  $I_0$ .

Figure 6 shows  $R_0$  as a function of  $V_s$  for irradiated p-strip detectors. The resistance increases with the fluence and reaches  $\sim 100 \text{ k}\Omega\text{cm}$ . The resistance is even larger for the detectors with  $4 \text{ k}\Omega\text{cm}$  resistivity.

The detector current will increase to  $\sim 0.5 \text{ mA}$  after 10 years of operation. The voltage drop across the above resistance is then  $\sim 50 \text{ V}$ , which has to be over biased. Comparing the designed maximum operation voltage of  $350 \text{ V}$ ,  $\sim 50 \text{ V}$  is at a marginal level, provided that  $R$  is not much different from  $R_0$ . If we intend to operate the detectors further longer, the ultimate detector lifetime is determined by the thermal runaway which happens at leakage current of  $\sim 2 \text{ mA}$  [13]. The voltage drop reaches  $200 \text{ V}$  in this extreme case, which certainly requires re-designing of the overall biasing system.

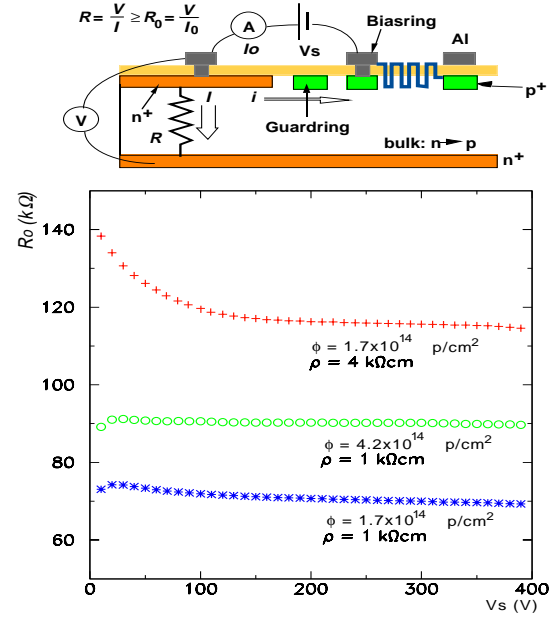


Figure 6: Edge resistance of irradiated detectors as a function of source voltage. The measurement configuration is shown above.

## IV. DISCUSSIONS

We compare the performance of various detector samples through the maximum collected charge  $Q_{\text{max}}$  and the correlation between C-V and charge collection curves. The shape of the charge collection curve is characterized by the voltage,  $V_Q(95\%)$ , where 95% of  $Q_{\text{max}}$  is accumulated. Similarly the C-V curve is characterized by the voltage,  $V_{1/C}(95\%)$ , at 95% of the plateau in  $1/C$ , which is supposed to be proportional to the depletion thickness and hence the charge generation. We corrected for the detector thickness and the data are expressed corresponding to  $300 \mu\text{m}$  thickness. The results are summarized in Table 3. The leakage current in the table is at  $V_Q(95\%)$  and expressed at  $-10^\circ\text{C}$ .

The voltages  $V_{1/C}(95\%)$  are systematically larger than  $V_Q(95\%)$ . The correlation between the two is plotted in Figure 7. As can be seen,  $V_{1/C}(95\%)$  is substantially lower than  $V_Q(95\%)$  for p-strip detectors, whereas the deviations are moderate for n-strip detectors. C-V curves are often used to

estimate the operation voltage. It is, however, obvious from the plot that irradiated p-strip (n-strip) detectors require much higher voltage by roughly 70% (20%) to achieve sufficiently high charge collection. At  $1.7 \times 10^{14}$  protons/cm<sup>2</sup>, there is small difference in terms of  $V_Q(95\%)$  between the two Hamamatsu p-on-n detectors with 1 k $\Omega$ cm and 4 k $\Omega$ cm bulk (H4pk and H1pk), and p-on-n detector fabricated in modified process (Hp4km). For SINTEF detectors (Sp4k-17 and Sp4k-42),  $V_Q(95\%)$  is ~20% larger than that of Hamamatsu detectors (Hp4k-17 and Hn4k-42).

Table 3

Summary of detector performance. The detector thickness is corrected and the values are for 300  $\mu$ m. The 95% voltages in charge collection of Sp4k-42 and Hn4k-42 were not reliably determined as described in the text.

Detector	$Q_{\max}$ 1=3.2 fC	95% Voltage (V)		$I_{\text{leak}}$ [ $\mu$ A]
		Charge collection	1/C	
Hp4k-0	1	47	62	0.004
Hn4kID-0	1.03	65	51	0.02
Hp4k-17	0.87	195	119	460
Hp1k-17	0.85	168	77	570
Hp4km-17	0.80	222	77	500
Sp4k-17	0.77	231	140	510
Hn4kID-17	1.00	218	158	700
Hn4kFC-17	0.99	261	197	630
Hn4kIA-17	0.93	269	189	950
Hn4kIB-17	0.99	256	243	610
Hp1k-42	0.70	402	215	860
Hn4kID-42	0.93	~300	309	~820
Sp4k-42	0.71	~500	290	~1020

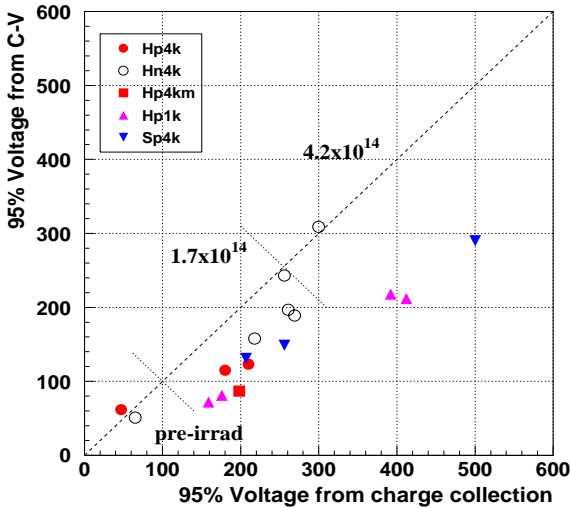


Figure 7: Correlation between 95% voltage in charge collection and that in 1/C.

The maximum collected charge  $Q_{\max}$  is plotted in Figure 8 as a function of proton fluence. The charge decreases with the fluence at a rate of ~2% per  $10^{14}$  protons/cm<sup>2</sup> for Hn4k, and of ~8% for Hp1k and Sp4k detectors. Although the Hp4k data at  $4.2 \times 10^{14}$  protons/cm<sup>2</sup> is not available and the two data points scatter at  $1.7 \times 10^{14}$ , Hp4k is consistent with Hp1k and Sp4k. There is small difference in the bulk resistivity and in the manufacturers as far as the drop in the charge collection is concerned.

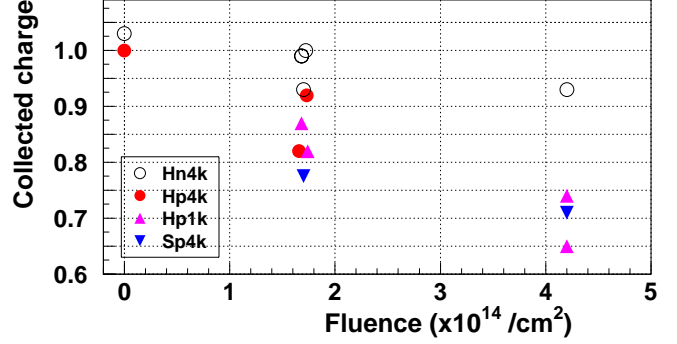


Figure 8: Maximum collected charge as a function of proton fluence.

We note that the leakage current at  $V_Q(95\%)$ ,  $I_{\text{leak}}$ , is systematically larger for n-strip detectors. This can be attributed to the effects of micro-discharge. Among the two new p-stop configurations, Hn4kIA draws a large current and Hn4kIB shows the smallest current. In the design of Hn4kIA, the region between the p-stop implants can accumulate the charge because poly-silicon plates do not exist on top.

#### IV. SUMMARY

We have fabricated various types of silicon microstrip detectors and irradiated them with 12-GeV protons to fluences of  $1.7 \times 10^{14}$  or  $4.2 \times 10^{14}$  protons/cm<sup>2</sup>. We evaluated the detector performances through I-V and C-V curves, and charge collection, and by probing the coupling capacitors. The results obtained in the present studies can be summarized as follows:

- The coupling capacitors are barely broken by irradiation. At  $1.7 \times 10^{14}$  protons/cm<sup>2</sup>, at most 1.5% of strips became faulty whereas most of the detectors showed 0 or 1 strip to be damaged out of 768 strips.
- The leakage current of n-strip detectors is in general larger than of p-strip detectors. A new p-stop configuration of Hn4kIB is promising in reducing the leakage current.
- There is small difference in initial p-on-n and n-on-n detectors in view of the shape in the charge collection curves. The charge collection of irradiated p-strip detectors remains as high as that of n-strip detectors at voltages lower than the full depletion voltage.
- The difference in initial resistivity 1 k $\Omega$ cm or 4 k $\Omega$ cm is small at the voltage where 95% of charge is collected. However at lower voltages, more charge can be collected for

1 k $\Omega$ cm detectors at  $1.7 \times 10^{14}$  protons/cm<sup>2</sup>. This difference becomes smaller at  $4.2 \times 10^{14}$  protons/cm<sup>2</sup>.

- The maximum collected charge decreases with the proton fluence at a rate 2% per  $10^{14}$  protons/cm<sup>2</sup> for n-strip detectors and ~8% for p-strip detectors. There is small difference in bulk resistivity and in the manufacturers in the maximum collected charge.
- Hamamatsu detectors made with modified n-side process showed performance equivalent to those made with conventional process.

## V. ACKNOWLEDGMENTS

The authors would like to acknowledge the cooperation of the beam channel and radiation safety groups of KEK. K. Takikawa and S. Kim of University of Tsukuba are also acknowledged for valuable suggestions. This work was supported by Japan Ministry of Education, Science and Culture.

## VI. REFERENCES

- [1] "ATLAS Inner Detector Technical Design Report", CERN/LHCC/97-17.
- [2] P. P. Allport *et al.*, "Radiation test of ATLAS full-sized n-in-n prototype detectors", Nucl. Instrum. And Methods A418 (1998) pp. 110-119.
- [3] Y. Unno *et al.*, "Evaluation of Radiation Damaged P-in-n and N-in-n Silicon Microstrip Detectors", submitted for IEEE Nucl. Sci. Symp., 1998.
- [4] E. Fretwurst *et al.* (RD2 Collab.), "Reverse annealing of the effective impurity concentration and long term operation scenario for silicon detectors in future collider experiments", Nucl. Instrum. And Methods A342 (1994) pp. 96-125.
- [5] H. J. Ziock *et al.*, "Temperature dependence of the radiation induced charge of depletion voltage in silicon PIN detectors", Nucl. Instrum. And Methods A342 (1994) pp. 96-104.
- [6] G. N. Taylor *et al.* (RD2 Collab.), "Radiation induced bulk damage in silicon detectors", Nucl. Instrum. and Methods A383 (1996) pp.144-154.
- [7] D. Pitzl *et al.*, "Type inversion in silicon detectors", Nucl. Instrum. and Methods A311 (1992) pp. 98-104.
- [8] Y. Unno *et al.*, "Novel P-stop Structure in the N-side Silicon Microstrip Detector", Talk given at "Hiroshima Symposium on Semiconductor Devices" at Melbourne 1997.
- [9] Y. Unno *et al.*, "Evaluation of P-stop Structures in the N-side of N-on-N Silicon Strip Detector", IEEE Trans. On Nucl. Sci. 45-3 (1998) pp. 401-405.
- [10] SINTEF Electronics and Cybernetics, Blindern, N-0314 Oslo, Norway.
- [11] S. Terada *et al.*, "Proton irradiation on p-bulk silicon detectors using 12 GeV PS at KEK", Nucl. Instrum. and Methods A383 (1996) pp. 159-165.
- [12] T. Taniguchi *et al.*, "New Electronics System for Silicon Strip Readout for 18 keV Electrons", IEEE Trans. on Nucl. Sci. 36 (1989) pp. 657-661.
- [13] A thermal simulation of the ATLAS barrel SCT module results that the thermal runaway occurs at heat generation of 220  $\mu$ W/mm<sup>2</sup> (at 0°C) in the detectors. See, T. Kondo, SDC Internal notes, INDET-NO-201 to 203.